NONLINEAR CONTROL OF AN ELECTRO-PNEUMATIC PROTECTION VALVE FOR CIRCUIT PRESSURE LIMITING

H. Németh, K. M. Hangos

Research Report SCL-005/2003

Nov 2003

Abstract

A simple feedforward nonlinear control design is presented in this report that is based on a simplified hybrid model of the electro-pneumatic protection valve used for circuit pressure limiting function of commercial vehicle air supply systems. First the model is analyzed according to the control design requirements with an emphasis on its hybrid behavior. The applied controller fulfils predefined optimality criteria that is achieved by numeric optimization methods.

Contents

1 Introduction

Lately the progression of electrical systems has been highly developed in the automotive sector. It has pushed many functions not realized before due to complexity. On the other hand cost reduction is another main driver. The new trend that the function is more and more packed into SW rather than into HW is even more growing. This enables more sophisticated functionality by less costs.

Protection valves are common parts in the brake system of commercial vehicles long time. However its function was always limited to its original aim. With introduction of electro-magnetic actuators to improve its original function additional tasks are also possible to be implemented. A possible additional function is the limiting of the circuit pressure according to dynamic set-point demands. This enables the omission of the conventional pressure limiting valves.

This report focuses on the model analysis and design of a controller that is able to fulfil circuit pressure limiting with use of an electro-pneumatic protection valve.

In recent papers [2, 3] an exhaustive modelling was done on the single circuit protection valve for control design purpose. This model was first developed from first engineering principles, which was obtained as an lumped hybrid index-1 model. This representation of the model was recognized too complex for control design purposes.

Therefore a model simplification was performed [4] to reduce the dimension of the state- and the parameter vector and the complexity of the equations. The simplification used L_2 performance norms to evaluate the error caused by the simplifying assumptions, which were made using engineering insight and operation experience on the behavior of the real system. The resulted simplified model preserved the engineering meaning of its variables and parameters, while the number of state variables and the number of parameters was reduced significantly.

The obtained simplified model was the object of model calibration and validation [5, 6]. The validated model fulfilled the predefined modelling error tolerances that serves as basis for model analysis and control design.

2 Nonlinear State-Space Model of the Electro-Pneumatic Protection Valve

2.1 System Description

The single circuit protection valve consists of the following elements (see Fig.1):

- **Input chamber** (1) This chamber has an input air flow from the compressor and two output flows towards the protection valve and the magnet valve.
- **Output chamber** (2) This chamber has an input air flow from the protection valve and an output towards the brake system or other consumers.
- **Control chamber** (3) This chamber has a single port that can be connected either to the input chamber or the ambient by the magnet valve.
- **Input piping** (4) It connects the input chamber to the protection valve.
- **Output piping** (5) This is the connection between the protection valve and the outlet chamber.
- **Protection valve** (6) The valve has an input connection from the input chamber through the input pipe and an output to the output chamber through the output pipe.
- **Control magnet valve** (7) It is a 3/2-way valve with solenoid excitation with one input port connected to the input chamber and two output ports. The one is going to the control chamber and the other one is exhausting to the environment.

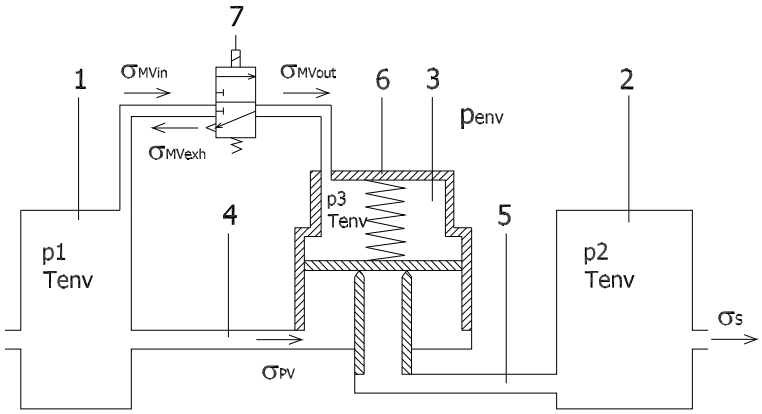

Figure 1: Schematic of single electro-magnetic protection valve with the important variables

2.2 Model Equations

According to the results of the model simplification the system variables are formed as follows:

State Vector The state vector includes the pressures of the control- and output chambers, speed and position of the two moving elements and the solenoid current as:

$$\mathbf{x} = \left[\begin{array}{ccccccc} p_2 & p_3 & x_{PV} & v_{PV} & x_{MV} & v_{MV} & I_{MV} \end{array} \right]^T. \tag{1}$$

Disturbance Vector The disturbance vector has the input chamber pressure, circuit air consumption as key disturbances and the environment temperature as slowly changing disturbances:

$$\mathbf{d} = \left[\begin{array}{ccc} p_1 & \sigma_S & T_{\text{env}} \end{array} \right]^T. \tag{2}$$

Input Vector The input vector includes one member only, which is the excitation voltage of the magnet valve:

$$\mathbf{u} = [U]. \tag{3}$$

Measured Output The measurable state variables and disturbances are formed as measured output including the three pressures and the solenoid current and circuit air consumption presence as discrete variable:

$$\mathbf{y} = \left[\begin{array}{ccccc} p_2 & p_3 & I & p_1 & \lambda_S \end{array} \right]^T. \tag{4}$$

2.2.1 State Equation

The simplified state space model is obtained as follows:

$$\begin{bmatrix} \dot{p}_2 \\ \dot{p}_3 \\ \dot{x}_{PV} \\ \dot{v}_{PV} \\ \dot{x}_{MV} \\ \dot{v}_{MV} \\ \dot{I} \end{bmatrix} = \begin{bmatrix} f_1(\mathbf{x}(t), \mathbf{d}(t)) \\ f_2(\mathbf{x}(t), \mathbf{d}(t)) \\ f_3(\mathbf{x}(t), \mathbf{d}(t)) \\ f_4(\mathbf{x}(t), \mathbf{d}(t)) \\ f_5(\mathbf{x}(t), \mathbf{d}(t)) \\ f_6(\mathbf{x}(t), \mathbf{d}(t)) \\ f_7(\mathbf{x}(t), \mathbf{d}(t)) \end{bmatrix} + \begin{bmatrix} 0 \\ 0 \\ 0 \\ 0 \\ 0 \\ 0 \\ \frac{(R_{ML} + \frac{x_{MV}}{\mu_0 A_{MB}})}{N^2} \end{bmatrix} u(t), \tag{5}$$

where the nonlinear state functions with all constitutive relations substituted are as:

$$f_1(\mathbf{x}(t),\mathbf{d}(t)) = \frac{\mathsf{R}T_{env}}{V_2}\left(\frac{\alpha_{PV} d_2 \pi x_{PVmax} p_1 \xi(p_1,p_2)}{1+e^{-u_{PV}(x_{PV}-x_{PVmax}/2)}} - \sigma_S\right), \tag{6}$$

$$f_2(\mathbf{x}(t),\mathbf{d}(t)) = \frac{\mathsf{R}T_{env}}{V_3}\left(\frac{\alpha_{MV} {d_{MVin}}^2 \pi p_1 \xi(p_1,p_3)}{4+4e^{-u_{MV}(x_{MVmax/2-x_{MV}})}} - \frac{\alpha_{MV} {d_{MVexh}}^2 \pi p_3 \zeta(p_3)}{4+4e^{-u_{MV}(x_{MV}-x_{MVmax/2})}}\right), \tag{7}$$

$$f_3(\mathbf{x}(t),\mathbf{d}(t)) = v_{PV}, \tag{8}$$

$$f_4(\mathbf{x}(t),\mathbf{d}(t)) = \frac{\frac{p_1}{4}\left(d_1^2-d_2^2\right)\pi + \frac{p_2}{4}d_2^2\pi - \frac{p_3}{4}d_1^2\pi - \mathsf{c}_{PV}(x_{PV}+x_{0PV}) - \mathsf{k}_{PV}v_{PV}}{m_{PV}}. \tag{9}$$

$$f_5(\mathbf{x}(t),\mathbf{d}(t)) = v_{MV}, \tag{10}$$

$$f_6(\mathbf{x}(t),\mathbf{d}(t)) = \frac{\frac{N^2I^2}{2(R_{ML}+\frac{x_{MV}}{\mu_0 A_{MB}})^2\mu_0 A_{MB}} - c_{MV}(x_{MV}+x_{0MV}) - \mathsf{k}_{MV}v_{MV}}{m_{MV}}, \tag{11}$$

$$f_7(\mathbf{x}(t),\mathbf{d}(t)) = \frac{Iv_{MV}}{(R_{ML}+\frac{x_{MV}}{\mu_0 A_{MB}})\mu_0 A_{MB}} - \frac{RI(R_{ML}+\frac{x_{MV}}{\mu_0 A_{MB}})}{N^2}, \tag{12}$$

where

$$\xi(p_1,p_2) = \sqrt{\frac{2\kappa\left(\left(\frac{p_2}{p_1}\right)^{\frac{2}{\kappa}} - \left(\frac{p_2}{p_1}\right)^{\frac{\kappa+1}{\kappa}}\right)}{(\kappa-1)\mathsf{R}T_{env}}}, \tag{13}$$

$$\xi(p_1,p_3) = \sqrt{\frac{2\kappa\left(\left(\frac{p_3}{p_1}\right)^{\frac{2}{\kappa}} - \left(\frac{p_3}{p_1}\right)^{\frac{\kappa+1}{\kappa}}\right)}{(\kappa-1)\mathsf{R}T_{env}}}, \tag{14}$$

$$\zeta(p_3) = \sqrt{\frac{2\kappa\left(\Pi_{crit}^{\frac{2}{\kappa}} - \Pi_{crit}^{\frac{\kappa+1}{\kappa}}\right)}{(\kappa-1)\mathsf{R}T_{env}}}. \tag{15}$$

2.2.2 Output Equation

The measured output is written as the following state-affine equation:

$$\mathbf{y} = \begin{bmatrix} 1 & 0 & 0 & 0 & 0 & 0 & 0 \\ 0 & 1 & 0 & 0 & 0 & 0 & 0 \\ 0 & 0 & 0 & 0 & 0 & 0 & 1 \\ 0 & 0 & 0 & 0 & 0 & 0 & 0 \\ 0 & 0 & 0 & 0 & 0 & 0 & 0 \end{bmatrix} \mathbf{x} + \begin{bmatrix} 0 \\ 0 \\ 0 \\ p_1 \\ \mathrm{sgn}(\sigma_S) \end{bmatrix}. \tag{16}$$

The performance output is generated from the measured output by the following simple equation:

$$\mathbf{z} = \begin{bmatrix} 1\ 0\ 0\ 0\ 0 \end{bmatrix} \mathbf{y}. \tag{17}$$

2.3 Hybrid Approach

The system contains several parts that exhibit discrete behavior. This means, that the equations, which describe the dynamic behavior of the corresponding subsystem vary according to certain circumstances as discussed by [7] (discrete-continuous model definition).

This implies that the above described equations refer to a dedicated hybrid state only. Some parts may change in different domains of the state space.

The simplified model contains three subsystems comprising hybrid properties: (i) protection valve piston and (ii) magnet valve armature due to stroke limitation having three hybrid states each and the (iii) protection valve/magnet valve air flow part due to sonic/subsonic streaming features including six hybrid states.

2.4 Operation Domain

During the experimental investigations the protection valve the following operation domain can be realized in terms of state-, input- and disturbance vectors. The state vector members are restricted as follows:

$$\begin{array}{ccc} 10^5 \leq p_2 \leq 1.3 \cdot 10^6 \text{ [Pa]}, & 10^5 \leq p_3 \leq 1.3 \cdot 10^6 \text{ [Pa]}, & 0 \leq x_{PV} \leq 0.002 \text{ [m]}, \\ -1 \leq v_{PV} \leq 1 \text{ [m/s]}, & 0 \leq x_{MV} \leq 0.0005 \text{ [m]}, & -1 \leq v_{MV} \leq 1 \text{ [m/s]}, \\ 0 \leq I \leq 1 \text{ [A]}. & & \end{array}$$

The input variable has the the following limits:

$$0 \leq U \leq 24 \text{ [V]}.$$

The disturbance variables are limited by the following constraints:

$$10^5 \leq p_1 \leq 1.3 \cdot 10^6 \text{ [Pa]}, \quad 0 \leq \sigma_S \leq 0.05 \text{ [kg/s]}, \quad 288 \leq T_{env} \leq 303 \text{ [K]}.$$

3 Dynamic Model Analysis

3.1 Nonlinear Input-affine State Equations

The nonlinear state equations transformed into intensive variable form described in Eqs. (5)–(12) can be expressed in a special format called input-affine state equation as [7]:

$$\frac{d\mathbf{x}}{dt} = f(\mathbf{x}) + g(\mathbf{x})u(t). \tag{18}$$

Observe that the $g(\mathbf{x})$ depends linearly on the state vector that is the effect of the input is bilinear to the time derivative of the state vector. Furthermore the last member is the only different from zero.

3.2 Hybrid Analysis

The above presented model includes an important property that state functions are piecewise defined depending on certain operating variables. These state functions, however, are continuous even on the boundary of two different hybrid operation domains and are continuously differentiable within these domains. Having done a systematic model simplification the the number of these hybrid parts and the overall number of hybrid states are drastically reduced. The final model includes three hybrid parts. Two of them represents the stroke limiting behavior of the moving elements and the third one is coupled with air flows. It is important to note that these parts exhibit their hybrid behavior independently of each other.

The first phenomenon containing hybrid behavior is the stroke limitation of the protection valve piston. This involves a linear stiff spring model on both sides when the piston stroke exceeds the limits, otherwise no such addition is included. The three state functions are as follows.

Hybrid-State 1a when $x_{PV} < 0$:

$$f_4(\mathbf{x}(t), \mathbf{d}(t)) = \frac{\frac{p_1}{4}\left(d_1^2 - d_2^2\right)\pi + \frac{p_2}{4}d_2^2\pi - \frac{p_3}{4}d_1^2\pi - \mathsf{c}_{PV}(x_{PV} + x_{0PV}) - \mathsf{k}_{PV}v_{PV} - c_{PVlim}x_{PV}}{m_{PV}}, \quad (19)$$

Hybrid-State 2a when $0 \leq x_{PV} \leq x_{PVmax}$:

$$f_4(\mathbf{x}(t), \mathbf{d}(t)) = \frac{\frac{p_1}{4}\left(d_1^2 - d_2^2\right)\pi + \frac{p_2}{4}d_2^2\pi - \frac{p_3}{4}d_1^2\pi - \mathsf{c}_{PV}(x_{PV} + x_{0PV}) - \mathsf{k}_{PV}v_{PV}}{m_{PV}}, \quad (20)$$

Hybrid-State 3a when $x_{PV} > x_{PVmax}$:

$$f_4(\mathbf{x}(t), \mathbf{d}(t)) = \frac{\frac{p_1}{4}\left(d_1^2 - d_2^2\right)\pi + \frac{p_2}{4}d_2^2\pi - \frac{p_3}{4}d_1^2\pi - \mathsf{c}_{PV}(x_{PV} + x_{0PV}) - \mathsf{k}_{PV}v_{PV} - c_{PVlim}(x_{PV} - x_{PVmax})}{m_{PV}}. \quad (21)$$

The second hybrid part is associated with the magnet valve armature stroke limitation that is very similar to the stroke limitation of the protection valve piston. The three state functions are obtained as:

Hybrid-State 1b when $x_{MV} < 0$:

$$f_6(\mathbf{x}(t), \mathbf{d}(t)) = \frac{\frac{N^2I^2}{2(R_{ML} + \frac{x_{MV}}{\mu_0 A_{MB}})^2 \mu_0 A_{MB}} - c_{MV}(x_{MV} + x_{0MV}) - \mathsf{k}_{MV}v_{MV} - c_{MVlim}x_{MV}}{m_{MV}}, \quad (22)$$

Hybrid-State 2b when $0 \leq x_{MV} \leq x_{MVmax}$:

$$f_6(\mathbf{x}(t), \mathbf{d}(t)) = \frac{\frac{N^2I^2}{2(R_{ML} + \frac{x_{MV}}{\mu_0 A_{MB}})^2 \mu_0 A_{MB}} - c_{MV}(x_{MV} + x_{0MV}) - \mathsf{k}_{MV}v_{MV}}{m_{MV}}, \quad (23)$$

Hybrid-State 3b when $x_{MV} > x_{MVmax}$:

$$f_6(\mathbf{x}(t), \mathbf{d}(t)) = \frac{\frac{N^2I^2}{2(R_{ML} + \frac{x_{MV}}{\mu_0 A_{MB}})^2 \mu_0 A_{MB}} - c_{MV}(x_{MV} + x_{0MV}) - \mathsf{k}_{MV}v_{MV} - c_{MVlim}(x_{MV} - x_{MVmax})}{m_{MV}}, \quad (24)$$

Observe that these hybrid states are depending on the associated strokes (x_{PV} and x_{MV}) only. Since the c_{PVlim} and c_{MVlim} constants have much higher values than the associated c_{PV} and c_{MV} spring stiffnesses this stroke limiting model is called stiff in its mathematical meaning.

The third part is jointly coupled with the airflows of the protection- and the magnet valve. The resulted six state functions are obtained as:

Hybrid-State 1c when $1 \geq \frac{p_2}{p_1} > \Pi_{crit}$ and $1 \geq \frac{p_3}{p_1} > \Pi_{crit}$:

$$f_1(\mathbf{x}(t), \mathbf{d}(t)) = \frac{\mathsf{R}T_{env}}{V_2} \left(\frac{\alpha_{PV} d_2 \pi x_{PVmax} p_1}{1 + e^{-u_{PV}(x_{PV} - x_{PVmax}/2)}} \sqrt{\frac{2\kappa \left(\left(\frac{p_2}{p_1}\right)^{\frac{2}{\kappa}} - \left(\frac{p_2}{p_1}\right)^{\frac{\kappa+1}{\kappa}} \right)}{(\kappa - 1)\mathsf{R}T_{env}}} - \sigma_S \right), \tag{25}$$

$$f_2(\mathbf{x}(t), \mathbf{d}(t)) = \frac{\mathsf{R}T_{env}}{V_3} \left(\frac{\alpha_{MV} {d_{MVin}}^2 \pi p_1}{4 + 4e^{-u_{MV}(x_{MVmax/2 - x_{MV}})}} \sqrt{\frac{2\kappa \left(\left(\frac{p_3}{p_1}\right)^{\frac{2}{\kappa}} - \left(\frac{p_3}{p_1}\right)^{\frac{\kappa+1}{\kappa}} \right)}{(\kappa - 1)\mathsf{R}T_{env}}} - \right.$$

$$\left. - \frac{\alpha_{MV} {d_{MVexh}}^2 \pi p_3}{4 + 4e^{-u_{MV}(x_{MV} - x_{MVmax/2})}} \sqrt{\frac{2\kappa \left(\Pi_{crit}^{\frac{2}{\kappa}} - \Pi_{crit}^{\frac{\kappa+1}{\kappa}} \right)}{(\kappa - 1)\mathsf{R}T_{env}}} \right), \tag{26}$$

Hybrid-State 2c when $\frac{p_2}{p_1} \leq \Pi_{crit}$ and $1 \geq \frac{p_3}{p_1} > \Pi_{crit}$:

$$f_1(\mathbf{x}(t), \mathbf{d}(t)) = \frac{\mathsf{R}T_{env}}{V_2} \left(\frac{\alpha_{PV} d_2 \pi x_{PVmax} p_1}{1 + e^{-u_{PV}(x_{PV} - x_{PVmax}/2)}} \sqrt{\frac{2\kappa \left(\Pi_{crit}^{\frac{2}{\kappa}} - \Pi_{crit}^{\frac{\kappa+1}{\kappa}} \right)}{(\kappa - 1)\mathsf{R}T_{env}}} - \sigma_S \right), \tag{27}$$

$$f_2(\mathbf{x}(t), \mathbf{d}(t)) = \frac{\mathsf{R}T_{env}}{V_3} \left(\frac{\alpha_{MV} {d_{MVin}}^2 \pi p_1}{4 + 4e^{-u_{MV}(x_{MVmax/2 - x_{MV}})}} \sqrt{\frac{2\kappa \left(\left(\frac{p_3}{p_1}\right)^{\frac{2}{\kappa}} - \left(\frac{p_3}{p_1}\right)^{\frac{\kappa+1}{\kappa}} \right)}{(\kappa - 1)\mathsf{R}T_{env}}} - \right.$$

$$\left. - \frac{\alpha_{MV} {d_{MVexh}}^2 \pi p_3}{4 + 4e^{-u_{MV}(x_{MV} - x_{MVmax/2})}} \sqrt{\frac{2\kappa \left(\Pi_{crit}^{\frac{2}{\kappa}} - \Pi_{crit}^{\frac{\kappa+1}{\kappa}} \right)}{(\kappa - 1)\mathsf{R}T_{env}}} \right), \tag{28}$$

Hybrid-State 3c when $1 \geq \frac{p_2}{p_1} > \Pi_{crit}$ and $\frac{p_3}{p_1} \leq \Pi_{crit}$:

$$f_1(\mathbf{x}(t), \mathbf{d}(t)) = \frac{\mathsf{R}T_{env}}{V_2} \left(\frac{\alpha_{PV} d_2 \pi x_{PVmax} p_1}{1 + e^{-u_{PV}(x_{PV} - x_{PVmax}/2)}} \sqrt{\frac{2\kappa \left(\left(\frac{p_2}{p_1}\right)^{\frac{2}{\kappa}} - \left(\frac{p_2}{p_1}\right)^{\frac{\kappa+1}{\kappa}} \right)}{(\kappa - 1)\mathsf{R}T_{env}}} - \sigma_S \right), \tag{29}$$

$$f_2(\mathbf{x}(t), \mathbf{d}(t)) = \frac{\mathsf{R}T_{env}}{V_3} \left(\frac{\alpha_{MV} {d_{MVin}}^2 \pi p_1}{4 + 4e^{-u_{MV}(x_{MVmax/2 - x_{MV}})}} \sqrt{\frac{2\kappa \left(\Pi_{crit}^{\frac{2}{\kappa}} - \Pi_{crit}^{\frac{\kappa+1}{\kappa}} \right)}{(\kappa - 1)\mathsf{R}T_{env}}} - \right.$$

$$-\frac{\alpha_{MV}{d_{MVexh}}^2\pi p_3}{4+4e^{-u_{MV}(x_{MV}-x_{MVmax/2})}}\sqrt{\frac{2\kappa\left(\Pi_{crit}^{\frac{2}{\kappa}}-\Pi_{crit}^{\frac{\kappa+1}{\kappa}}\right)}{(\kappa-1)\mathsf{R}T_{env}}}\Bigg), \tag{30}$$

Hybrid-State 4c when $\frac{p_2}{p_1} \leq \Pi_{crit}$ and $\frac{p_3}{p_1} \leq \Pi_{crit}$:

$$f_1(\mathbf{x}(t),\mathbf{d}(t)) = \frac{\mathsf{R}T_{env}}{V_2}\left(\frac{\alpha_{PV}d_2\pi x_{PVmax}p_1}{1+e^{-u_{PV}(x_{PV}-x_{PVmax}/2)}}\sqrt{\frac{2\kappa\left(\Pi_{crit}^{\frac{2}{\kappa}}-\Pi_{crit}^{\frac{\kappa+1}{\kappa}}\right)}{(\kappa-1)\mathsf{R}T_{env}}}-\sigma_S\right), \tag{31}$$

$$f_2(\mathbf{x}(t),\mathbf{d}(t)) = \frac{\mathsf{R}T_{env}}{V_3}\left(\frac{\alpha_{MV}{d_{MVin}}^2\pi p_1}{4+4e^{-u_{MV}(x_{MVmax/2-x_{MV}})}}\sqrt{\frac{2\kappa\left(\Pi_{crit}^{\frac{2}{\kappa}}-\Pi_{crit}^{\frac{\kappa+1}{\kappa}}\right)}{(\kappa-1)\mathsf{R}T_{env}}}-\right.$$
$$\left.-\frac{\alpha_{MV}{d_{MVexh}}^2\pi p_3}{4+4e^{-u_{MV}(x_{MV}-x_{MVmax/2})}}\sqrt{\frac{2\kappa\left(\Pi_{crit}^{\frac{2}{\kappa}}-\Pi_{crit}^{\frac{\kappa+1}{\kappa}}\right)}{(\kappa-1)\mathsf{R}T_{env}}}\right), \tag{32}$$

Hybrid-State 5c when $1 \geq \frac{p_2}{p_1} > \Pi_{crit}$ and $1 > \frac{p_1}{p_3} > \Pi_{crit}$:

$$f_1(\mathbf{x}(t),\mathbf{d}(t)) = \frac{\mathsf{R}T_{env}}{V_2}\left(\frac{\alpha_{PV}d_2\pi x_{PVmax}p_1}{1+e^{-u_{PV}(x_{PV}-x_{PVmax}/2)}}\sqrt{\frac{2\kappa\left(\left(\frac{p_2}{p_1}\right)^{\frac{2}{\kappa}}-\left(\frac{p_2}{p_1}\right)^{\frac{\kappa+1}{\kappa}}\right)}{(\kappa-1)\mathsf{R}T_{env}}}-\sigma_S\right), \tag{33}$$

$$f_2(\mathbf{x}(t),\mathbf{d}(t)) = \frac{\mathsf{R}T_{env}}{V_3}\left(\frac{-\alpha_{MV}{d_{MVin}}^2\pi p_1}{4+4e^{-u_{MV}(x_{MVmax/2-x_{MV}})}}\sqrt{\frac{2\kappa\left(\left(\frac{p_1}{p_3}\right)^{\frac{2}{\kappa}}-\left(\frac{p_1}{p_3}\right)^{\frac{\kappa+1}{\kappa}}\right)}{(\kappa-1)\mathsf{R}T_{env}}}-\right.$$
$$\left.-\frac{\alpha_{MV}{d_{MVexh}}^2\pi p_3}{4+4e^{-u_{MV}(x_{MV}-x_{MVmax/2})}}\sqrt{\frac{2\kappa\left(\Pi_{crit}^{\frac{2}{\kappa}}-\Pi_{crit}^{\frac{\kappa+1}{\kappa}}\right)}{(\kappa-1)\mathsf{R}T_{env}}}\right), \tag{34}$$

Hybrid-State 6c when $\frac{p_2}{p_1} \leq \Pi_{crit}$ and $1 > \frac{p_1}{p_3} > \Pi_{crit}$:

$$f_1(\mathbf{x}(t),\mathbf{d}(t)) = \frac{\mathsf{R}T_{env}}{V_2}\left(\frac{\alpha_{PV}d_2\pi x_{PVmax}p_1}{1+e^{-u_{PV}(x_{PV}-x_{PVmax}/2)}}\sqrt{\frac{2\kappa\left(\Pi_{crit}^{\frac{2}{\kappa}}-\Pi_{crit}^{\frac{\kappa+1}{\kappa}}\right)}{(\kappa-1)\mathsf{R}T_{env}}}-\sigma_S\right), \tag{35}$$

$$f_2(\mathbf{x}(t),\mathbf{d}(t)) = \frac{\mathsf{R}T_{env}}{V_3}\left(\frac{-\alpha_{MV}{d_{MVin}}^2\pi p_1}{4+4e^{-u_{MV}(x_{MVmax/2-x_{MV}})}}\sqrt{\frac{2\kappa\left(\left(\frac{p_1}{p_3}\right)^{\frac{2}{\kappa}}-\left(\frac{p_1}{p_3}\right)^{\frac{\kappa+1}{\kappa}}\right)}{(\kappa-1)\mathsf{R}T_{env}}}-\right.$$

$$\left.-\frac{\alpha_{MV}{d_{MVexh}}^2\pi p_3}{4+4e^{-u_{MV}(x_{MV}-x_{MVmax/2})}}\sqrt{\frac{2\kappa\left(\Pi_{crit}^{\frac{2}{\kappa}}-\Pi_{crit}^{\frac{\kappa+1}{\kappa}}\right)}{(\kappa-1)\mathsf{R}T_{env}}}\right), \tag{36}$$

These state functions are paired so they are dependent hybrid states due to the common p_1 disturbance variable included into the pressure ratio dependence into both hybrid conditions.

The properties of these six hybrid states can be summarized as follows:

- The oddly numbered hybrid states have subsonic streaming property in the first state function (f_1)
- The evenly numbered hybrid states have sonic streaming property in the first state function (f_1)
- The hybrid states 1c and 2c have subsonic streaming property in the first term (σ_{MVin}) of the second state function (f_2)
- The hybrid states 3c and 4c have sonic streaming property in the first term (σ_{MVin}) of the second state function (f_2)
- The hybrid states 5c and 6c have subsonic streaming property with negative streaming direction in the first term (σ_{MVin}) of the second state function (f_2)

Since the governing conditions of the above presented three hybrid parts are different terms from each other, the included hybrid states are independent hybrid states in the three different groups.

The above state space model is a set of ordinary differential equations (ODEs), where all the state functions are explicitly defined in all the hybrid states (there are no algebraic constrains on the state variables). Moreover, all the hybrid states define smooth state functions on the boundary of the corresponding hybrid domain. This means, that derivative of the state variables are piecewise defined continuous functions as the system transits from one hybrid state to another, i.e. *the state variables are smooth functions in at least first order.*

3.2.1 Hybrid State Transitions

The state transitions of a hybrid part defines which are the possible transitions that can occur driven by the inputs of the system if the system is in the corresponding hybrid state.

The first two hybrid parts have three hybrid states each where a sequential state transition can occur driven by the manipulable input. This means that all the a- and b- hybrid states can be governed by the input voltage.

The state transition diagrams of the protection valve piston and magnet valve armature stroke limitation can be see in Fig. 2.

The third hybrid part that defines the state equations of the chamber pressures varies depending on the input considered there. If all the system inputs (manipulable and uncontrollable, i.e. disturbances) are considered, then all the hybrid states can be reached from any other one. Its hybrid state transition graph is seen in Fig. 3. If the manipulable input is considered only, then only four hybrid states are triggered. The corresponding state transition diagram can be seen in Fig. 4.

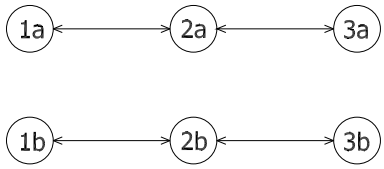

Figure 2: State transition graphs of the protection- and magnet valve stroke limiting

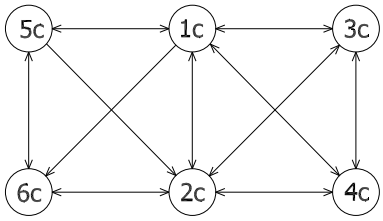

Figure 3: State transition graph of the air flow hybrid part considering all inputs

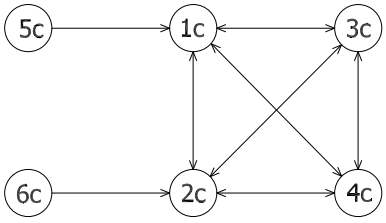

Figure 4: State transition graph of the air flow hybrid part considering manipulable input only

3.2.2 State Reachable Property

The state reachable property of the modelled system is strongly coupled with state transition diagrams discussed in the last sections.

A hybrid system is called (hybrid state) controllable or reachable if one can always find an appropriate input function to move the system from its given initial hybrid state to a specified final state in finite time [7]. This applies to every given initial state final state pairs. This means, when the state transition graph as a directed graph is in itself a strongly connected component then the underlying system is reachable. Note that a directed graph is a strongly connected component in itself if there is at least one directed path from any vertex to any other vertex.

In conclusion, the first two hybrid parts show reachable property because the appropriate input function can always be found that moves the system from one hybrid state to the other one, moreover no deadlocks are found.

The state transition graph of the third hybrid part shows that the states 5c and 6c are not triggered directly by the manipulable input, just the rest of the hybrid states (1c–4c), which form a strongly connected components in themselves. However, this is not a problem because the target operation domain of a controller candidate is entirely covered by the triggered hybrid states (1c–4c). This is imposed by a target that the controller should be able to decrease the control pressure down to the environment pressure and to increase up to the input pressure level. Higher control pressure (that is covered by hybrid states 5c and 6c) than the input pressure can occur by quick drop of the input pressure but it is not a required operation range of the control pressure. Deadlocks are not found in this hybrid part, too.

3.3 Local nonlinear controllability, controllability distribution

To check nonlinear local controllability in the neighborhood of a given $\mathbf{x}_0$ operation point one should prepare the controllability distribution of the system.

Since the system has a single output only the f and g functions are both vector valued with dimension of 7. This implies that one should compute at least the first 7 steps of the controllability distribution (Δ_c) algorithm [1] to check whether it spans the state space in each point in the operating region. Moreover each step should consider the check of singular points.

The algorithm starts with $\Delta_0 = \text{span}\{g\}$. This distribution has the dimension of 1 that has no singularity since g is linear function of $\mathbf{x}$. The next steps calculates k-th distribution as follows:

$$\Delta_k = \Delta_{k-1} + \sum_{i=0}^{m} [g_i, \Delta_{k-1}], \tag{37}$$

where m, the number of inputs, is 1 in our case. The last term, the Lie-bracket is calculated as $[f, g]$ for Δ_1 that can be expanded as follows:

$$[f, g] = \frac{\partial g}{\partial \mathbf{x}} f - \frac{\partial f}{\partial \mathbf{x}} g = g_{\mathrm{x}} f - f_{\mathrm{x}} g. \tag{38}$$

The calculation stops where the distribution does not change anymore (i.e. $\Delta_{k^*} = \Delta_{k^*+1} \equiv \Delta_c$). The g_{x} term gives a quite simple and constant sparse matrix because of the linear property of $g(\mathbf{x})$ as follows:

$$g_{\mathrm{x}} = \begin{bmatrix} 0 & 0 & 0 & 0 & 0 & 0 & 0 \\ 0 & 0 & 0 & 0 & 0 & 0 & 0 \\ 0 & 0 & 0 & 0 & 0 & 0 & 0 \\ 0 & 0 & 0 & 0 & 0 & 0 & 0 \\ 0 & 0 & 0 & 0 & 0 & 0 & 0 \\ 0 & 0 & 0 & 0 & 0 & 0 & 0 \\ 0 & 0 & 0 & 0 & \frac{1}{N^2 \mu_0 A_{MB}} & 0 & 0 \end{bmatrix}. \tag{39}$$

Considering the complexity f and the hybrid parts included there the higher level distributions (Δ_1 and above) are complex expressions with many pathes because of the hybrid properties. Due to this fact the controllability distribution is not examined. Later controllability is covered by structural properties.

3.4 Structural Properties

Structural properties hold for a class of system with the same structure. Structure indices define the size of the structural variables of a system. The four structure indices n, m, r and v defines the size of the following system variables:

$$\mathbf{x}(t) \in \mathbb{R}^n, \mathbf{y}(t) \in \mathbb{R}^m, \mathbf{u}(t) \in \mathbb{R}^r, \mathbf{d}(t) \in \mathbb{R}^v. \tag{40}$$

The dimension of structure matrices, analogous to the LTI system matrices, are defined by the above structure indices as follows:

$$[\mathbf{A}] \in \mathbb{R}^{n \times n}, [\mathbf{B}] \in \mathbb{R}^{n \times r}, [\mathbf{C}] \in \mathbb{R}^{m \times n}, [\mathbf{D}] \in \mathbb{R}^{m \times r}, [\mathbf{E}] \in \mathbb{R}^{n \times v}, [\mathbf{F}] \in \mathbb{R}^{m \times v}, \tag{41}$$

where the matrix $[\mathbf{E}]$ denotes the transfer from the disturbance to the state vector and the matrix $[\mathbf{F}]$ is the transfer from the disturbance to the output.

The structure of a general matrix $\mathbf{W}$ is given by the structure matrix $[\mathbf{W}]$ whose entries are defined as follows [7]:

$$[w]_{ij} = \begin{cases} 0 & \text{if } w_{ij} = 0, \\ * & \text{otherwise,} \end{cases} \tag{42}$$

where $*$ is a nonzero undetermined entry.

For some structural dynamical properties like structural stability one may need to note the sign of the matrix entries. For this purpose the structural signed matrices are defined (denoted by $\{\mathbf{W}\}$ for a general matrix $\mathbf{W}$), where the element are defines as:

$$[w]_{ij} = \begin{cases} 0 & \text{if } w_{ij} = 0, \\ - & \text{if } w_{ij} < 0, \\ + & \text{if } w_{ij} > 0. \end{cases} \tag{43}$$

The structure matrices of a nonlinear input-affine state space model are obtained from the linearized model, i.e. the effect of a state variable to state function is obtained that must be determined in the whole operation domain.

The structure matrices of the single electro-pneumatic protection valve model are as follows:

$$[\mathbf{A}] = \begin{bmatrix} 0/* & 0 & * & 0 & 0 & 0 & 0 \\ 0 & * & 0 & 0 & * & 0 & 0 \\ 0 & 0 & 0 & * & 0 & 0 & 0 \\ * & * & * & * & 0 & 0 & 0 \\ 0 & 0 & 0 & 0 & 0 & * & 0 \\ 0 & 0 & 0 & 0 & * & * & * \\ 0 & 0 & 0 & 0 & * & * & * \end{bmatrix}, [\mathbf{B}] = \begin{bmatrix} 0 \\ 0 \\ 0 \\ 0 \\ 0 \\ 0 \\ * \end{bmatrix}, [\mathbf{C}] = \begin{bmatrix} * & 0 & 0 & 0 & 0 & 0 & 0 \\ 0 & * & 0 & 0 & 0 & 0 & 0 \\ 0 & 0 & 0 & 0 & 0 & 0 & * \\ 0 & 0 & 0 & 0 & 0 & 0 & 0 \\ 0 & 0 & 0 & 0 & 0 & 0 & 0 \end{bmatrix}, \tag{44}$$

$$[\mathbf{D}] = \begin{bmatrix} 0 \\ 0 \\ 0 \\ 0 \\ 0 \end{bmatrix}, [\mathbf{E}] = \begin{bmatrix} * & * & * \\ * & 0 & * \\ 0 & 0 & 0 \\ * & 0 & 0 \\ 0 & 0 & 0 \\ 0 & 0 & 0 \\ 0 & 0 & 0 \end{bmatrix}, [\mathbf{F}] = \begin{bmatrix} 0 & 0 & 0 \\ 0 & 0 & 0 \\ 0 & 0 & 0 \\ * & 0 & 0 \\ 0 & * & 0 \end{bmatrix}. \tag{45}$$

The signed structure matrices are calculated as:

$$\{\mathbf{A}\} = \begin{bmatrix} 0/+ & 0 & ? & 0 & 0 & 0 & 0 \\ 0 & ? & 0 & 0 & ? & 0 & 0 \\ 0 & 0 & 0 & + & 0 & 0 & 0 \\ + & - & - & - & 0 & 0 & 0 \\ 0 & 0 & 0 & 0 & 0 & + & 0 \\ 0 & 0 & 0 & 0 & ? & - & + \\ 0 & 0 & 0 & 0 & ? & + & ? \end{bmatrix}, \{\mathbf{B}\} = \begin{bmatrix} 0 \\ 0 \\ 0 \\ 0 \\ 0 \\ 0 \\ + \end{bmatrix}, \{\mathbf{C}\} = \begin{bmatrix} + & 0 & 0 & 0 & 0 & 0 & 0 \\ 0 & + & 0 & 0 & 0 & 0 & 0 \\ 0 & 0 & 0 & 0 & 0 & 0 & + \\ 0 & 0 & 0 & 0 & 0 & 0 & 0 \\ 0 & 0 & 0 & 0 & 0 & 0 & 0 \end{bmatrix}, \tag{46}$$

$$\{\mathbf{D}\} = \begin{bmatrix} 0 \\ 0 \\ 0 \\ 0 \\ 0 \end{bmatrix}, \{\mathbf{E}\} = \begin{bmatrix} ? & - & + \\ ? & 0 & ? \\ 0 & 0 & 0 \\ + & 0 & 0 \\ 0 & 0 & 0 \\ 0 & 0 & 0 \\ 0 & 0 & 0 \end{bmatrix}, \{\mathbf{F}\} = \begin{bmatrix} 0 & 0 & 0 \\ 0 & 0 & 0 \\ 0 & 0 & 0 \\ + & 0 & 0 \\ 0 & + & 0 \end{bmatrix}, \tag{47}$$

with ? denoting either +, 0 or − , i.e. unknown.

Note that the first entry of the state structure matrix changes depending on the hybrid state the system is working in (it is 0 in 2c, 4c and 6c hybrid states otherwise $*$). All other structure matrix entries are hybrid state-invariant.

The first important property of the state structure matrix is the presence of full structural rank regardless the value of the altering entry.

Using the block matrix [**A B**] one can conclude that the system is *structurally (state) controllable* due to the full rank with the exception of null measure sets [7]. This is a hybrid state-invariant property of the system.

Similarly the rank of block matrix $[\mathbf{C}\ \mathbf{A}]^T$ gives that the investigated system is *structurally (state) observable* as of having full rank with the same exception of null measure sets [7]. This feature is also not depending on the altering entry of the state structure matrix.

Based on the structure matrices of the system the structure graph can be prepared that describes the complete interaction between the entries of the system variables. The structure graph is depicted in Fig.5, where the double circle denotes the input variable, triangles are the disturbance entries, single circles are the state variable terms and rectangles are used for output entries.

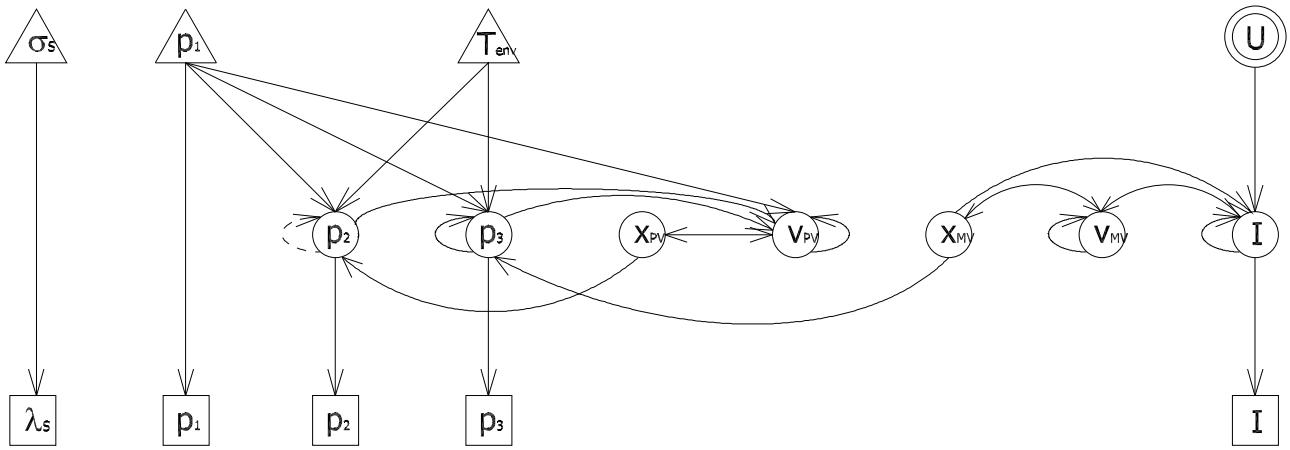

Figure 5: Structure graph of the single circuit protection valve

Using the state structure matrix and structure graph of the system, the relative degree of the system can also be determined [1]. The relative degree is exactly equal to the number of times one has to differentiate the output $\mathbf{y}(t)$ in order that the input $\mathbf{u}(t)$ appears in the equation.

In case of MIMO systems the relative degree is given to a predefined input-output pair. In this case it can be given for each output (that is coupled with the input) since the system has a single input only. The relative degree can be obtained from the structure graph by counting the directed pathes from the input to the given output variable.

Using the graph above the relative degree can be determined to the p_I, p_3 and p_2 outputs that are 1, 4, and 7 respectively. This way one can conclude that the investigated system is of *maximum relative degree* considering the performance output that is hybrid state-invariant.

3.5 Asymptotic Stability

A solution of the state equation is asymptotically stable if a neighboring solution, resulting from a perturbation and described by a different initial condition has the same limit as $t \to \infty$.

This means that a nonlinear state space system with the initial condition for the state vector $q(0) = q_0^0$ giving rise to the nominal solution $q^0(t)$, $t \leq 0$. The nominal solution of the system is

asymptotically stable if whenever one takes another different initial condition q_0 such that $\|q_0 - q_0^0\| < \delta$ with $\delta > 0$ being sufficiently small, then $\|q_0 - q_0^0\| \to 0$ if $t \to \infty$, where $q(t)$, $t \leq 0$ is the perturbed solution with initial condition $q(0) = q_0$.

The global asymptotic stability of the system can be proven by finding a Lyapunov-function, which is a dissipative scalar positive definite function. Quadratic Lyapunov function candidates can be used for the system to determine the domain of its asymptotic stability.

The investigated system shows *locally asymptotically stable* (open loop stable) behavior when its state variables are tending to the same values from any initial state considering constant input and disturbance variables. An important steady-state value of the system with respect to the pressure limiting control problem is when the initial conditions imply the opening state of the protection valve piston and zero input voltage is applied:

$$\mathbf{x}_{\text{lim}} = \begin{bmatrix} p_1 & p_{\text{env}} & x_{PV\max} & 0 & x_{MV\max} & 0 & 0 \end{bmatrix}^T. \tag{48}$$

Experimental step response tests shows that the valve system exhibits locally asymptotically stable behavior in a wide neighborhood of this steady-state value.

3.6 Disturbance Sensitivity Analysis

Disturbance sensitivity assessment is performed on each the disturbance signals. The aim is to identify members that has negligible impact on the model output and remove them from the candidate disturbance to be considered for the control.

To investigate the impact of disturbance signal change an output error metrics is defined and dedicated test cases are selected since the model is nonlinear in itself and in its parameters as well. This is similar like the one used for parameter sensitivity analysis [6].

3.6.1 Test Cases and Error Metrics

Four pressure limiting test cases, that are similar to a typical control cycle of circuit pressure limiting using a protection valve, are used for the sensitivity assessment. The first three test cases investigate the short term dynamic behavior with two test pulses of different duration (deactivations are 90, 100 and 110ms long respectively). The fourth one checks the long term dynamics with one test pulse (deactivation is 90ms long). The input voltage in these test cases are depicted in Fig. 6.

The sensitivity assessment is made one-by-one on the disturbances, where only one disturbance value is changed and the output of this modified model is compared to the original one. All the disturbance signal have constant values over the time.

Individual errors are calculated for each test case based on the entries of the output vector of the single protection valve as follows:

$$\begin{aligned} \varepsilon_{p_2} &= \sqrt{\frac{1}{T}\int_0^T \left(\frac{p_2(t) - p_{2s}(t)}{\overline{p_2}}\right)^2 dt}, \\ \varepsilon_{p_3} &= \sqrt{\frac{1}{T}\int_0^T \left(\frac{p_3(t) - p_{3s}(t)}{\overline{p_3}}\right)^2 dt}, \\ \varepsilon_I &= \sqrt{\frac{1}{T}\int_0^T \left(\frac{I(t) - I_s(t)}{\overline{I}}\right)^2 dt}, \end{aligned} \tag{49}$$

where the suffix $_s$ refers to the corresponding output vector entries of the modified disturbance, the overline refers to the integrate mean of the signal and T is the duration of the test case. Each individual error is an Euclidian signal norm of the error in the particular output compared to response of the

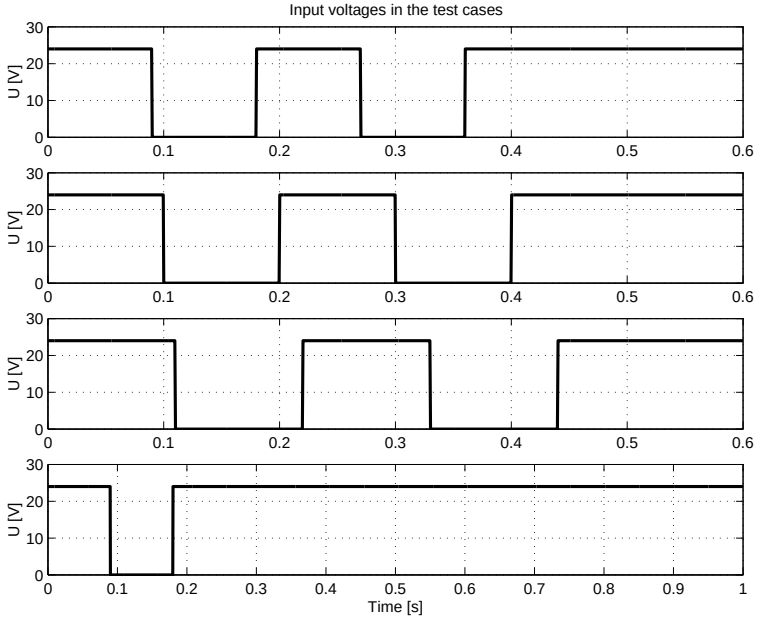

Figure 6: Input voltage profile of the test cases

original model. A partial error is calculated based on these individual error terms for each test case as:

$$\varepsilon_{\text{Partial}} = \sqrt{\varepsilon_{p_2}^2 + \varepsilon_{p_3}^2 + \varepsilon_I^2}, \tag{50}$$

This error shows the total error of the corresponding test case. Finally the average error is calculated on the individual errors of the four test cases using the Root Mean Square (RMS) as follows:

$$\varepsilon_{\text{Total}} = \sqrt{\frac{1}{4}\sum_{k=1}^{4}\left(\varepsilon_{p_2,k}^2 + \varepsilon_{p_3,k}^2 + \varepsilon_{I,k}^2\right)}, \tag{51}$$

where the index k refers to the corresponding testing case.

3.6.2 Sensitivity Evaluation

All the investigated disturbances are modified with -10 and +10 percents from their original values, although one exception needed to be done, since the relative range of the T_{env} signal is only about 5 percent of its mean value. Due to this reason this signal is modified by -2.5 and +2.5 percents that covers its whole operation range. If the total error remains below the pre-specified tolerance of 2 percent in case of both directions the model is found not sensitive to the change of that signal. The results of the sensitivity assessment are shown in Table 1.

Table 1: Sensitivity of the model to partially known parameters

Parameter	ε_{Total} [%]		Sensitivity
	-10 (2.5) %	+10 (2.5)%	
p_1	12.0784	12.1071	Sensitive
σ_S	5.6371	5.7957	Sensitive
T_{env}	0.74062	0.74019	Not sensitive

The sensitivity results of the disturbance signals show that the input pressure and brake system air consumption signals have a big impact on model error so these signal are important inputs of the controller.

4 Feedforward Bang-Bang Controller Design

4.1 Control Aims

The following control aims are considered for circuit pressure limiting function of the electro-pneumatic protection valve:

$\mathcal{C}1$. The circuit pressure has to be limited according to a static set point pressure with $5 \cdot 10^4$ Pa tolerance.

$\mathcal{C}2$. The pressure breakdown caused by the external air consumption in the circuit should be minimized.

$\mathcal{C}3$. The control has to be robust with respect to the parameters of the simplified model.

4.2 Control Constraint: Two-level Input

There is an important constraint applied to the system input that influences the type of the controller. The input voltage can take two levels only. This is imposed by the simple electronic actuator (transistor) connected to the solenoid valve, which can switch on or off the supply voltage to the solenoid. The level of input voltage in switch on phase is determined by the supply voltage, in off phase it is switched to the ground.

The above constraint implies that the controller should be a member of the bang-bang controller family, where the manipulable variable is the actuation time.

4.3 Disturbance Observation

Having investigated the sensitivity of the model by the disturbance vector members the result shows that the model is sensitive to the air consumption (σ_S) and input pressure (p_1) disturbance signals. The last term (T_{env}) does not produce a significant effect on the output variables, moreover its operation range is small and the change of this disturbance signal is definitely slow (some K per hour) compared to the processes in the protection valve.

Based on these results one can conclude that the first two disturbance terms (σ_S, p_1) are key information for the pressure limiter controller as having high effect and considerable dynamic behavior.

Since from the key disturbances only one (p_1) is directly measurable while the other is known in terms of an indicator discrete signal only (λ_S – practically the presence of the consumption), the σ_S signal needs to be estimated from the measurable signals using an observer.

The high relative degree of the system and the a priori unknown duration of the air consumption implies that the pressure limiting control problem for avoiding overshoots is not causal with respect to the air consumption disturbance signal. Therefore a restricted version of the problem is investigated further.

Besides of restricting the problem to a causal one by simplifying assumptions, these assumptions below ensure the above mentioned observer structure simple:

$\mathcal{A}1$. The air consumption caused by the brake system is constant over time during a single brake intervention.

$\mathcal{A}2$. The duration of the air consumption is constant.

In this restricted case the observation can be based on the initial part of a brake intervention when the air consumption is already present ($\lambda_S = 1$) but the protection valve piston is still closed. The closed piston state is obtained from Eq.9, meanwhile the pressure derivative of the output chamber is only affected by the external air consumption in Eq.6, because the first term between the brackets is zero under closed piston position.

4.4 Control Principle

As the control problem is basically the rejection of the disturbance made by external air consumption, a *fixed programme feedforward control* was considered. The control design consists of two steps.
(i) The input profile applied to the system is obtained by off line step response optimizations that considers the control aims and the input constraint assuming fixed levels of the major disturbances. From the results a fixed input programme table is constructed.
(ii) The signals of the measured output are then used to determine the actual input programme to fulfil the control aims.

The fixed programme table is divided into 11 parts according to the values of the considered two disturbance signals (σ_s, p_1). The air consumption signal range is equally divided into 4 parts along the operation domain of the signal, while the input pressure signal range is also divided into 4 parts but unequally, the pressure range below the set point plus overshoot tolerance ($(9.5 + 0.5) \cdot 10^5$ Pa) forms one part (P1 programme). Above this pressure level three equally divided parts are made. The programme table layout is shown in Tab.2.

Table 2: Layout of the Fixed Programme Table

		p_1 [Pa]			
		$< 10^6$	10^6	$1.15 \cdot 10^6$	$1.3 \cdot 10^6$
σ_S [kg/s]	0	P1	P2		
	0.016		P3	P4	P5
	0.033		P6	P7	P8
	0.05		P9	P10	P11

P1 programme includes full magnet valve release (opened protection valve during air consumption presence), P2 programme has full magnet valve excitation (closed protection valve during air consumption presence). The other programmes include individual input voltage profiles obtained from the off line optimization.

The appropriate fixed programme is selected based on the air consumption estimated by the observer and on the measured input pressure. The nearest lower air consumption is selected, while the nearest upper input pressure gives the actual fixed programme. These considerations are made to avoid the overshoot rather than the undershoot. The scheme of the closed loop system is depicted in Fig.7.

4.5 The Optimization Problem

This section describes how an element program P_i in the fixed programme table is determined by off-line optimization.

4.5.1 Optimization Method

The control design target can be mathematically formulated according to the predefined control aims as the following cost functional to be minimized:

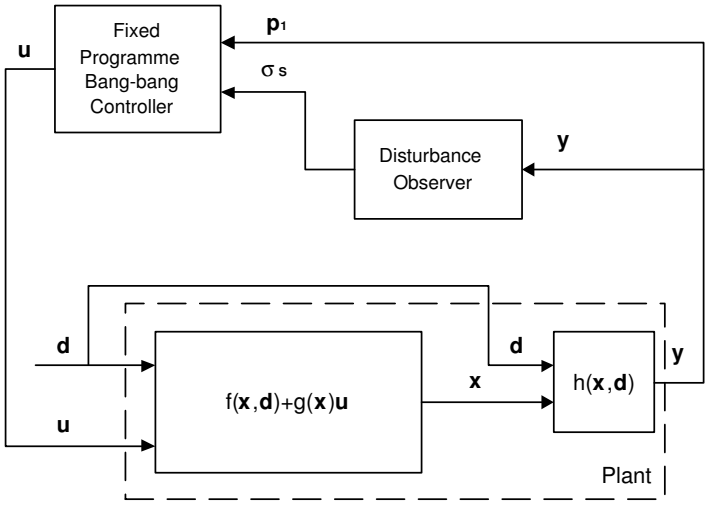

Figure 7: Block scheme of the closed loop system

$$\mathcal{J}(\mathbf{z},\mathbf{u}) = \int_0^\infty \left(Q(\Delta\mathbf{z})\Delta\mathbf{z}^2 + S\left(\frac{\mathrm{d}\mathbf{u}}{\mathrm{d}t}\right)^2 \right) dt \tag{52}$$

where $\Delta\mathbf{z} = \mathbf{z} - \mathbf{z}_{set}$ is the performance output set point deviation, $\frac{\mathrm{d}\mathbf{u}}{\mathrm{d}t}$ is the time-derivative of the input, $Q(\Delta\mathbf{z})$ is the performance output error weighting function and S is an input weighting scalar.

Both Q and S are positive definite. The performance output error weighting function is used to penalize the overshoot more intensively than the break down in the following piecewise defined form:

$$Q(\Delta\mathbf{z}) = \begin{cases} \mathrm{e}^{a\Delta\mathbf{z}} & \text{if } \Delta\mathbf{z} > 0, \\ 1 & \text{otherwise.} \end{cases} \tag{53}$$

The parameter a is set so that the weight at the maximal prescribed overshoot is 5.

With the above cost function and the constraint made on the input variable the problem can be solved by discrete numeric optimization. For this purpose the simplex search algorithm [8] was used. The considered input actuation time interval was 400 ms. This interval was evenly divided into 10 and 25 segments (i.e. each segment was 40 ms and 16 ms long respectively), where the input voltage given to the system in the corresponding segment could be 0 V or the supply voltage (24 V). By increasing the number of the input time interval divisions one can obtain more accurate setup of the performance output after the transient phase, but it is more demanding from numeric optimization point of view because of the more possible local minimum loci. The considered constant duration of the air consumption was 250 ms.

4.5.2 Optimization Results

Fig.9 shows optimized model responses for two cases. The input voltage profile for the individual fixed programmes are shown in Tab.4, where 0 refers to the off phase and 1 to the on phase of the input voltage. The model parameter setup used for the simulation calculations is seen in Tab.5.

In conclusion the properties of the obtained input programmes are as follows. In case of low input pressure (P3, P4 and P5) a single long off-block followed by an on-block are applied. As the input pressure increases considering the same air consumption the first on-intervention shifts to an earlier segment (e.g. P9 vs. P10). As the air consumption gets higher assuming the same input pressure level the first on-intervention shifts to later (e.g. P8 vs. P11).

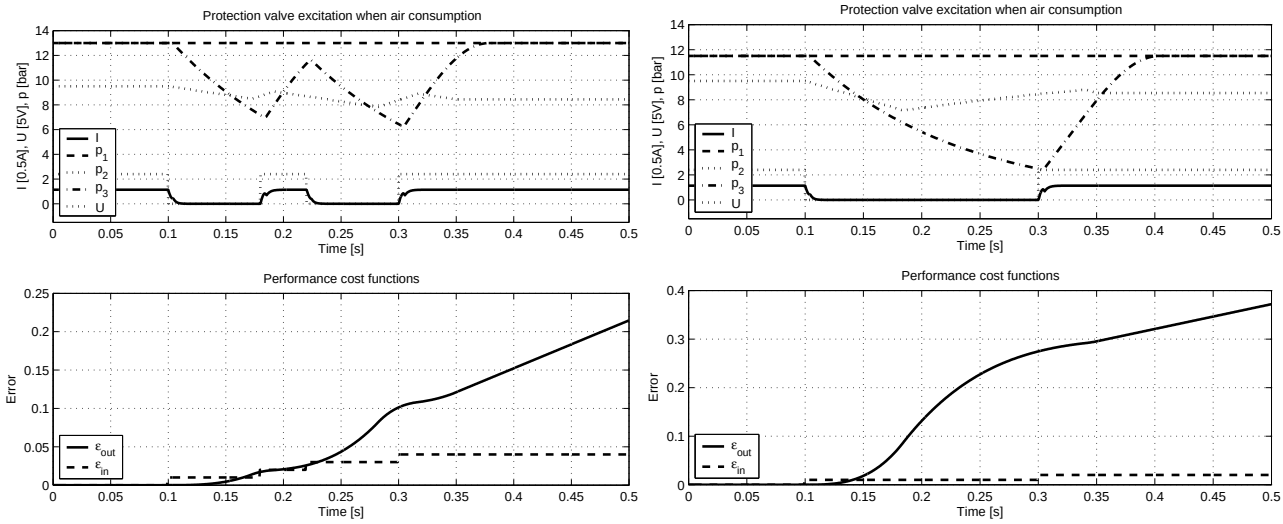

Figure 8: Two response functions obtained by optimizations (P5 and P7 programmes) in the 10 division case

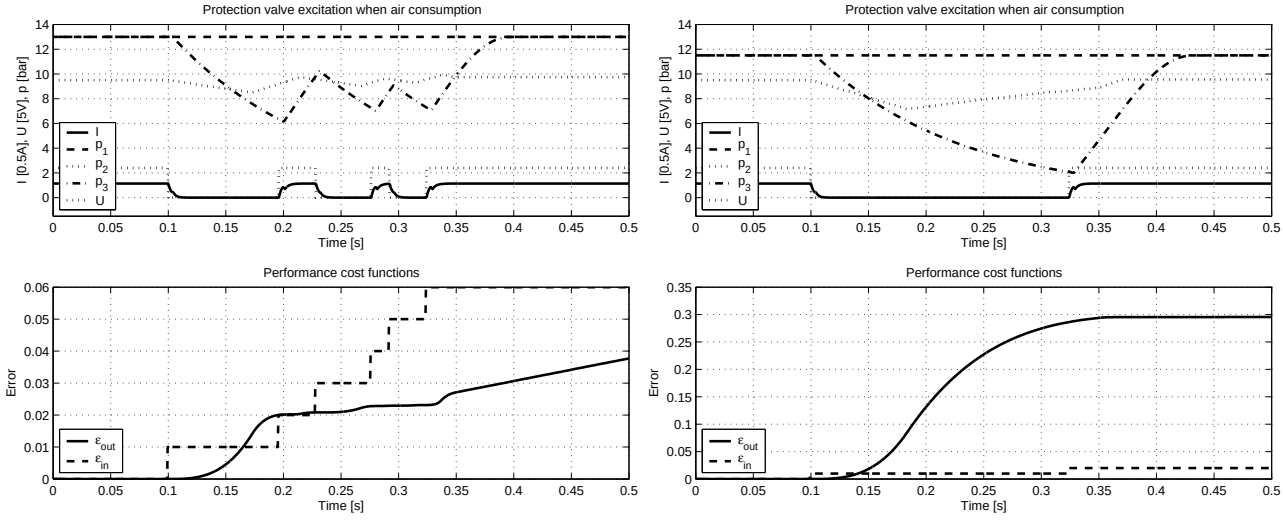

Figure 9: Two response functions obtained by optimizations (P5 and P7 programmes) in the 25 division case

Table 3: Input entries of the individual fixed programmes for 10 division case

Prg.	Input Segments									
	1	2	3	4	5	6	7	8	9	10
P1	0	0	0	0	0	0	0	0	0	0
P2	1	1	1	1	1	1	1	1	1	1
P3	0	0	0	0	0	1	1	1	1	1
P4	0	0	1	0	0	0	1	1	1	1
P5	0	0	1	0	0	1	1	1	1	1
P6	0	0	0	0	0	0	0	1	1	1
P7	0	0	0	0	0	1	1	1	1	1
P8	0	0	0	0	1	0	1	1	1	1
P9	0	0	0	0	0	0	0	0	0	1
P10	0	0	0	0	0	0	0	0	1	1
P11	0	0	0	0	0	0	1	1	1	1

Table 4: Input entries of the individual fixed programmes for 25 division case

Prg.	Input Segments																								
	1	2	3	4	5	6	7	8	9	10	11	12	13	14	15	16	17	18	19	20	21	22	23	24	25
P1	0	0	0	0	0	0	0	0	0	0	0	0	0	0	0	0	0	0	0	0	0	0	0	0	0
P2	1	1	1	1	1	1	1	1	1	1	1	1	1	1	1	1	1	1	1	1	1	1	1	1	1
P3	0	0	0	0	0	0	0	0	0	0	0	0	0	1	1	1	1	1	1	1	1	1	1	1	1
P4	0	0	0	0	0	0	0	1	1	0	0	0	1	1	1	1	1	1	1	1	1	1	1	1	1
P5	0	0	0	0	0	0	1	1	0	0	0	1	0	0	1	1	1	1	1	1	1	1	1	1	1
P6	0	0	0	0	0	0	0	0	0	0	0	0	0	0	0	0	0	1	1	1	1	1	1	1	1
P7	0	0	0	0	0	0	0	0	0	0	0	0	0	0	1	1	1	1	1	1	1	1	1	1	1
P8	0	0	0	0	0	0	0	0	0	0	0	1	1	1	0	0	1	1	1	1	1	1	1	1	1
P9	0	0	0	0	0	0	0	0	0	0	0	0	0	0	0	0	0	0	0	0	0	0	1	1	1
P10	0	0	0	0	0	0	0	0	0	0	0	0	0	0	0	0	0	0	0	1	1	1	1	1	1
P11	0	0	0	0	0	0	0	0	0	0	0	0	0	0	0	0	1	1	1	1	1	1	1	1	1

5 Conclusions

A single circuit electro-pneumatic protection valve was investigated in this paper from control design point of view that is intended to be used for circuit pressure limiting.

A simplified nonlinear hybrid model containing three independent hybrid parts has first been analyzed for its dynamical properties. By analyzing the hybrid properties it was shown that all the hybrid states are reachable in the whole operation domain of the controller. It was also shown that the model is structurally state controllable and observable, and has maximum relative degree. These properties are invariant with respect to the hybrid states. The asymptotic open loop stability was also investigated.

Based on the control aims and input level restrictions a bang-bang control is proposed in feedforward operating mode. The applied input profiles are determined for different measured output signal ranges by optimization, which considered output deviation and input energy terms.

Acknowledgements

This work has been supported by the Hungarian Science Fund (OTKA) through grant $T042710$, which is gratefully acknowledged.

References

[1] A. Isidori. *Nonlinear Control Systems*. Springer, Berlin, 1995.

[2] Németh, H., Ailer, P., Hangos, K. M. (2002) *Nonlinear Hybrid Model of a Single Protection Valve for Pneumatic Brake Systems*, Research Report of Computer and Automation Research Institute, Budapest, Hungary, SCL-2/2002.

[3] Németh, H., Ailer, P., and Hangos, K. M. (2002) Nonlinear Modelling and Model Verification of a Single Protection Valve. *Periodica Polytechnica Ser. Transportation Eng.* Vol. 30, Budapest. 2002–30/1,2, pp. 69–92.

[4] Németh, H., Palkovics, L., Hangos, K. M. (2002) *Model Simplification of a Single Protection Valve; A Systematic Approach*, Research Report of Computer and Automation Research Institute, Budapest, Hungary, SCL-004/2002.

[5] Nmeth, H., Palkovics, L., Hangos, K. M. (2003) *System Identification of an Electro-Pneumatic Protection Valve*, Research Report of Computer and Automation Research Institute, Budapest, Hungary, SCL-001/2003.

[6] Nmeth, H., Hangos, K. (2003) Elektro-pneumatikus vdszelep rendszeridentifikcija, *Gp*, Miskolc, Hungary, 2003/3–4, pp. 33–42. (In Hungarian)

[7] Hangos, K. M. and Cameron, I. (2001) *Process Modelling and Model Analysis.* Process systems engineering Volume 4, Academic Press, London.

[8] Nelder, J. A. and Mead, R. (1965) A Simplex Method for Function Minimization. *Computer Journal*, Volume 7, pp. 308–313.

[9] Lagarias, J.C., J. A. Reeds, M. H. Wright, and P. E. Wright. (1998) Convergence Properties of the Nelder-Mead Simplex Method in Low Dimensions. *SIAM Journal of Optimization*, Vol. 9 Number 1, pp. 112–147.

[10] Dennis, J.E. Jr. and R.B. Schnabel. (1983) *Numerical Methods for Unconstrained Optimization and Nonlinear Equations*, Prentice Hall, Englewood Cliffs, N.J.

[11] *Optimization Toolbox, for Use with Matlab, User's Guide, Version 2.* (2000), The Mathworks Inc., Natick, MA, USA.

A Appendix - Nomenclature

Variables

a	pressure distribution factor [-;s/m]
A	area, surface [m^2]
α	contraction coefficient [-]
c	spring coefficient [N/m]
c	specific heat [J/kgK]
d	diameter [m]
ε	error [-]
F	force [N]
φ	angle [-]
I	electric current [A]
k	heat transmission coefficient [W/m^2K]
k	damping coefficient [Ns/m]
κ	adiabatic exponent [-]
L	inductance [Vs/A]
m	mass [kg]
σ	air flow [kg/s]
μ	permeability [Vs/Am]
N	solenoid turns [-]
p	absolute pressure [Pa]
R	resistance [electric-Ω; magnetic-A/Vs]
R	specific gas constant [J/kgK]
s	gas speed [m/s]
t	time [s]
T	absolute temperature [K]
U	voltage [V]
v	speed [m/s]
V	volume [m^3]
x	stroke [m]

Indices

$_0$	refers to initial state or vacuum
$_1$	refers to input chamber
$_2$	refers to output chamber
$_3$	refers to control chamber
$_{PV}$	refers to protection valve
$_{MV}$	refers to magnet valve
$_C$	refers to compressor
$_S$	refers to brake system
$_{env}$	refers to environment
$_v$	refers to constant volume
$_p$	refers to constant pressure
$_{in}$	refers to inlet
$_{out}$	refers to outlet
$_{exh}$	refers to exhaust
$_{max}$	refers to maximum
$_{lim}$	refers to limitation
$_\Sigma$	refers to magnetic resultant
$_{MP}$	refers to magnet valve plug part
$_{MF}$	refers to magnet valve frame
$_{MJ}$	refers to magnet valve jacket
$_{MB}$	refers to magnet valve body
$_{MC1}$	refers to magnet valve air clearance 1
$_{MC2}$	refers to magnet valve air clearance 2
$_{ML}$	refers to magnetic loop of constant members
$_{Partial}$	refers to partial term of one test case
$_{Total}$	refers to partial term of all test cases

B Appendix - Model Parameters

Table 5: Model parameters

Parameter name	**Symbol**	**Unit**	**Value**
Adiabatic exponent	κ	-	1.4
Permeability of vacuum	μ_0	Vs/Am	$4\pi \cdot 10^7$
Specific gas constant	R	J/kgK	287.14
Stiffness of MV spring	c_{MV}	N/m	1500
Stiffness of PV spring	c_{PV}	N/m	10000
Diameter of PV piston	d_1	m	0.018
Valve seat diameter of PV	d_2	m	0.01
MV armature diameter	d_{MB}	m	0.01
MV inlet port diameter	$d_{MV\text{in}}$	m	0.0007
MV exhaust port diameter	$d_{MV\text{exh}}$	m	0.0006
Mass of MV armature	m_{MV}	kg	0.002
Mass of PV piston	m_{PV}	kg	0.02
Number of solenoid turns	N	-	1500
Electric resistance of MV	R	Ω	42.16
MV cross section factor	u_{MV}	-	$2 \cdot 10^4$
PV cross section factor	u_{PV}	-	10^5
Output chamber volume	V_2	m^3	0.001
Control chamber volume	V_3	m^3	$5 \cdot 10^{-6}$
Spring preset stroke of MV	x_{MV0}	m	0.002
Maximal MV stroke	$x_{MV\text{max}}$	m	0.0005
Spring preset stroke of PV	x_{PV0}	m	0.009
Maximal PV stroke	$x_{PV\text{max}}$	m	0.002
MV contraction coefficient	α_{MV}	-	0.6834
PV contraction coefficient	α_{PV}	-	0.2966
Damping coefficient of MV	k_{MV}	Ns/m	2
Damping coefficient of PV	k_{PV}	Ns/m	10
Magnetic loop resistance	R_{ML}	A/Vs	$1.843 \cdot 10^7$